



Contents lists available at ScienceDirect

Global and Planetary Change

journal homepage: www.elsevier.com/locate/gloplacha

The medieval climate anomaly in Europe: Comparison of the summer and annual mean signals in two reconstructions and in simulations with data assimilation

Hugues Goosse^{a,*}, Joel Guiot^b, Michael E. Mann^c, Svetlana Dubinkina^a, Yoann Sallaz-Damaz^a

^a Université Catholique de Louvain, Earth and Life Institute, Georges Lemaître Centre for Earth and Climate Research, Chemin du Cyclotron, 2, B-1348 Louvain-la-Neuve, Belgium

^b CEREGE, Aix-Marseille Université/CNRS, Europole Méditerranéen de l'Arbois, Aix-en-Provence, France

^c Department of Meteorology and Earth and Environmental Systems Institute, Pennsylvania State University, University Park, USA

ARTICLE INFO

Article history:

Received 7 January 2011

Accepted 6 July 2011

Available online 20 July 2011

Keywords:

Europe

Last Millennium

seasonal climate signal

atmospheric circulation

data assimilation

ABSTRACT

The spatial pattern and potential dynamical origin of the Medieval Climate Anomaly (MCA, around 1000 AD) in Europe are assessed with two recent reconstructions and simulations constrained to follow those reconstructions by means of paleoclimate data assimilation. The simulations employ a climate model of intermediate complexity (LOVECLIM). The data assimilation technique is based on a particle filter using an ensemble of 96 simulations. The peak winter (and annual mean) warming during the MCA, in our analyses, is found to be strongest at high latitudes, associated with strengthened mid-latitude westerlies. Summer warmth, by contrast, is found to be greatest in southern Europe and the Mediterranean Sea, associated with reduced westerlies and strengthened southerly winds off North Africa. The results of our analysis thus underscore the complexity of the spatial and seasonal structure of the MCA in Europe.

© 2011 Elsevier B.V. All rights reserved.

1. Introduction

Europe is one region of the world for which a large number of proxy records are available spanning the past millennium (e.g. Lamb, 1965; Pfister et al., 1998; Klimentko et al., 2001; van Engelen et al., 2001; Shabalova and van Engelen, 2003; Charman, 2010; Guiot et al., 2010). The density of proxy records is particularly great in the Alps (e.g., Büntgen et al., 2005; Mangini et al., 2005; Büntgen et al., 2006; Corona et al., 2010) and in Fennoscandia (e.g. Briffa et al., 1992; Hiller et al., 2001; Tiljander et al., 2003; Kremenetski et al., 2004; Grudd, 2008; Seppa et al., 2009; Gunnarson et al., 2010). These proxy records generally indicate relatively warm conditions during Medieval Time, i.e. between roughly 850 and 1250 AD. This is particularly clear for summer as the majority of the proxies represent summer or growing season (April to September) temperature. However, the few direct estimates of winter and annual mean changes also indicate relatively mild conditions (e.g., Pfister et al., 1998; Van Engelen et al., 2001; Shabalova and van Engelen, 2003; Tiljander et al., 2003).

This has been one of the bases for the quite loose definition of the so-called Medieval Warm Period or Medieval Climate Anomaly (MCA, e.g., Lamb, 1965; Hughes and Diaz, 1994; Bradley et al., 2003). Nevertheless, Medieval warmth was certainly not continuous, nor was it spatially synchronous (e.g. Hughes and Diaz, 1994; Bradley et al., 2003; Goosse et al., 2005; Guiot et al., 2010). In particular, several records indicate cold conditions between 1050 and 1150 AD

(e.g. Büntgen et al., 2006; Grudd, 2008; Corona et al., 2010) with temperatures similar to those observed later, during what is often referred to as the Little Ice Age (LIA, roughly between 1400 and 1850).

The generally mild European conditions during the MCA could potentially be the consequence of a prolonged positive anomaly in external radiative forcing. Medieval Times are characterised by high Total Solar Irradiances (TSI) around 900–1000 and 1050–1250 (Bard et al., 2000; Muscheler et al., 2007; Delaygue and Bard, 2010) which should have contributed to observed surface warming. Major explosive volcanic eruptions cool the surface, in particular in summer, by reducing the incoming shortwave radiative heating (Robock, 2000; Fischer et al., 2007). The relative absence of major eruptions during the MCA relative to the later LIA (Crowley et al., 2003; Gao et al., 2008) thus also likely contributes to the level of warmth at that time. Additionally, Europe has been subject to major land use changes during the past millennium (Goudie, 1993; Pongratz et al., 2008; Kaplan et al., 2009). As deforestation increases the surface albedo (biogeophysical effect), this induces a general cooling tendency in Europe since Medieval Times (Brovkin et al., 2006; Goosse et al., 2006a; Pongratz et al., 2009). Deforestation also affects the surface characteristics governing the evapotranspiration and the heat and momentum exchanges between the atmosphere and the land surface. However, the net effect of those changes is usually harder to evaluate than the one of the albedo (Matthews et al., 2004; Feddema et al., 2005; Pitman et al., 2009). Finally, deforestation also has an impact on the global atmospheric CO₂ concentration (biogeochemical effect) inducing a large-scale warming that compensates in some regions for the cooling caused by the biogeophysical effect (Pongratz et al., 2010).

* Corresponding author. Tel.: +32 10 47 32 98; fax: +32 10 47 47 22.
E-mail address: hugues.goosse@uclouvain.be (H. Goosse).

In addition to these predominantly thermodynamic effects, volcanic and solar forcing can profoundly influence the large-scale atmospheric circulation. For instance, there is a tendency for the positive phase of the North Atlantic Oscillation (NAO) in the winter following a major volcanic eruption. Positive solar radiative forcing, similarly, is associated with the positive phase of the NAO. These effects imply a relatively complex regional spatial response, with either an amplification or damping of the direct radiatively-forced temperature responses depending on the region (Robock, 2000; Shindell et al., 2001, 2003; Fischer et al., 2007).

Finally, purely internal variability of the climate system can potentially play a dominant role in the climate changes observed at regional and continental scales during the past millennium (Goosse et al., 2005; Servonnat et al., 2010). The positive phase of the NAO leads to relatively warm winters over much of Europe due to the associated stronger onshore flow of warm maritime air off the Atlantic Ocean (Hurrell, 1995; Wanner et al., 2001; Trouet et al., 2009). Since much of Europe is under the influence of westerly winds, any change in sea surface temperature over the Atlantic, ocean (e.g. due to changes in oceanic circulation) can impart a strong imprint on temperatures in Europe through downstream advection (e.g. Sutton and Hodson, 2005; Pohlmann et al., 2006; Semenov et al., 2010). It has even been argued that internal variability alone might explain the observed temperature variations in Europe during pre-industrial times (Bengtsson et al., 2006). External forcing is however – at least for certain periods of the past millennium – a very likely contributor to the observed climate changes (e.g., Fischer et al., 2007; Hegerl et al., 2007, 2011).

As briefly summarised above, the mechanisms that might potentially explain the observed temperature changes in Europe over past centuries have been investigated in several studies. Those studies included analysis of paleoclimate reconstructions and the use of various types of climate models. Comparing model results with reconstructions to infer the dominant processes responsible for any particular observed change in climate is not straightforward however. Due to the chaotic nature of internal climate variability, it is exceedingly unlikely that any coupled climate model will be able to reproduce the precise realisation of past climate, i.e. will be able to fortuitously capture the actual phases of the various internal modes of climate variability, influencing for instance temperature patterns, without additional real-world constraints. Such constraints can be provided by the climate observations themselves. With the possible exception of a specific very strong external forcing scenario (e.g. Timmreck et al., 2009), models and data can compare only in a statistical sense (e.g.; Brewer et al., 2006). This is a quite strong limitation if one is interested in understanding the observed changes associated with a particular time period such as the MCA.

Complementary information can be obtained using paleoclimate data assimilation, combining model results and proxy climate observations to obtain an optimal estimate of the past states of the system (e.g., Widmann et al., 2010). Since data assimilation constrains the model to follow observations within their uncertainties, it provides an estimate of the full climate state, i.e. a suite of simulated atmospheric, oceanic and land variables, that is most compatible with the information in the proxy data. The method therefore allows for the investigation of specific hypotheses regarding the role of large-scale climate dynamics in explaining the paleo-observations (e.g.; van der Schrier and Barkmeijer, 2005; Crespin et al. 2009; Widmann et al., 2010).

In the present study, we use a particle filter data assimilation method (van Leeuwen, 2009). Two different recent surface temperature reconstructions (Mann et al., 2008, 2009; Guiot et al., 2010) are assimilated into the climate model LOVECLIM (Goosse et al., 2010a). One of the two reconstructions (Mann et al., 2009) estimates annual mean temperatures patterns across the globe for the last 1500 years, while the second (Guiot et al., 2010) estimates warm season

(i.e. growing season/summer) temperatures in Europe over the past 1400 years. Use of these dual reconstructions thus allows for an analysis of the seasonal characteristics of European temperature changes and their relationship with larger-scale climate changes over the past millennium.

The model, the proxy-based reconstructions, and the data assimilation method are briefly presented in Section 2. Section 3 describes and analyses the simulations of European climate during the MCA interval. We discuss our results in Section 4 before presenting our concluding remarks.

2. Experimental setup

In order to perform the simulations with data assimilation that will be used to study European climate, we have to select a model (Section 2.1), a forcing scenario (Section 2.2), initial conditions (Section 2.3), a data assimilation method (Section 2.4), proxy-based reconstructions (Section 2.5), and a way to measure the agreement between model results and the reconstruction (Section 2.6). Simplifications and assumptions are required on each of those steps. Many of them are imposed by technical constraints: the model must represent sufficiently well the physics of the system but must also be fast enough to apply data assimilation techniques; the number of simulation in an ensemble should be of the order of 100 at most because of computer-time limitation although a larger number might be suitable to precisely characterise variability at all spatial scales; the two spatial reconstructions, for two different seasonal ranges, that are available for our period of interest are based on a limited number of proxy records and on methods that may have biases. In order to formulate precisely the problem, an uncertainty must thus be a priori associated to all the important assumptions, as described in each of the sub-sections below. Despite those assumptions and uncertainties, we will show that our simulations with data assimilation bring new results compared to simulations without data assimilation and contribute to improve our knowledge of European climate during the MCA. This will be evaluated a posteriori by ensuring the compatibility of the results with our working hypotheses and by analysing the useful information brought in Sections 3 and 4.

2.1. The climate model

LOVECLIM 1.2 is a three-dimensional Earth system model of intermediate complexity that includes representations of the atmosphere, the ocean and sea ice, the land surface (including vegetation), the ice sheets, the icebergs and the carbon cycle. Goosse et al. (2010a) provide a comprehensive description of the current model version as well as a brief comparison of the simulation results with the observed climate both for present-day conditions and key past periods.

The atmospheric component is ECBilt2, a quasi-geostrophic model with T21 horizontal resolution (corresponding to about 5.6° by 5.6°) and 3-level on the vertical (Opsteegh et al., 1998). The ocean component is CLIO3 (Goosse and Fichefet, 1999), which consists of an ocean general circulation model coupled to a thermodynamic-dynamic sea-ice model. Its horizontal resolution is of 3° by 3°, and there are 20 levels in the ocean. ECBilt–CLIO is coupled to VECODE, a vegetation model that simulates the dynamics of two main terrestrial plant functional types, trees and grasses, as well as desert (Brovkin et al., 2002). Its resolution is the same as of ECBilt. In order to reduce the computational time requirements of the model and because of the focus of our study, the ice sheets, icebergs and carbon cycle components are not activated in our simulations. As a consequence, we cannot compute the time development of the atmospheric CO₂ concentration interactively or take into account explicitly the biogeochemical impacts of land use changes as, for instance, done in Pongratz et al. (2010) and Jungclaus et al. (2010).

Those effects are instead included through the greenhouse gas scenario applied in the model (see [Section 2.2](#)).

Because of its coarse resolution and of the simplifications introduced in the representation of some processes, LOVECLIM is much faster than the more sophisticated coupled climate models, allowing us to perform the large number of simulations required by data assimilation techniques. Moreover, it includes a sufficient description of the major processes responsible for past changes and shows reasonable results in the extra-tropics ([Goosse et al., 2010a](#)). Despite those simplifications, we have chosen to consider only one set of model parameterization and to not take into account any uncertainty on model parameters. This allows a simpler experimental design and previous experiments have shown that including such an uncertainty in model parameters does not have a major impact on our results with data assimilation for the Last Millennium ([Goosse et al., 2010b](#))

2.2. Forcing

The simulations discussed here are driven by both natural forcings (orbital, volcanic and solar) and anthropogenic forcings (changes in greenhouse gas concentrations, in sulphate aerosols and land use) in the same way as in [Goosse et al. \(2010a\)](#). The long-term changes in orbital parameters follow [Berger \(1978\)](#) and the long-term evolutions of greenhouse gas concentrations are imposed as in [Goosse et al. \(2005\)](#). The influence of anthropogenic (AD 1850–2000) sulphate aerosols is represented through a modification of surface albedo ([Charlson et al., 1991](#)). The forcing due to anthropogenic land-use changes (including surface albedo, surface evaporation and water storage modifications) is applied following [Ramankutty and Foley \(1999\)](#) as in [Goosse et al. \(2006a\)](#). Finally, natural external forcing due to variations in solar irradiance and explosive volcanism is prescribed following the reconstructions of [Crowley et al. \(2003\)](#) and [Muscheler et al. \(2007\)](#), respectively. The total solar irradiance changes have been scaled to provide an increase of 1 W m^{-2} between the Maunder minimum (late 17th century) and the late 20th century, corresponding to a radiative forcing at the top of the atmosphere of about 0.2 W m^{-2} ([Lean et al., 2002](#); [Foukal et al., 2006](#); [Gray et al., 2010](#)).

The forcing scenarios selected here are reasonable but alternative reconstructions are available, in particular for the land-use changes (e.g., [Pongratz et al., 2008](#), [Kaplan et al., 2009](#); [Gaillard et al., 2010](#)) as well as for the solar and volcanic forcings (see [Schmidt et al. \(2010\)](#) for a recent synthesis). The way we include the contribution of aerosols is rather crude and thus leads to large uncertainties. Furthermore, the magnitude of the solar forcing is still relatively uncertain, a recent reconstruction, for instance, arguing in favour of a much larger amplitude of past variations compared to the values selected here ([Shapiro et al., 2011](#)). As a consequence, a random component is added to the natural and anthropogenic forcings in all the members of a simulation with data assimilation in order to take into account the uncertainties in all the forcings. This random component, which is uncorrelated in time and between the members of the ensemble, follows a Gaussian probability distribution with a standard deviation of 0.4 W m^{-2} . We have selected this value as it is the order of magnitude of the difference between the various reconstructions of time filtered solar and volcanic forcings, in particular of the difference between the weak solar forcing applied here and the larger one applied in previous experiments such as the one included in the IPCC AR4 ([Jansen et al., 2007](#)). As this random component is applied at global scale through a modification of the total solar irradiance (leading thus to additional variation of the total solar irradiance with a standard deviation of about 2 W m^{-2}), it does not well represent the uncertainties associated with the regional impact of land-use changes, with a potential impact on our analysis (see [Section 4](#)).

2.3. Initial conditions

Using this forcing, an ensemble of 10 simulations without data assimilation has been performed over the period 501–2000 AD. The simulation driven by the [Mann et al. \(2009\)](#) reconstruction (hereafter referred to as ASSIM-MANN) covers the same period. The simulation with data assimilation driven by the [Guiot et al. \(2010\)](#) reconstruction (hereafter referred to as ASSIM-GUIOT) starts one century later to match the period covered by the reconstruction. The initial conditions in 501 AD and 601 AD are obtained from the results of a transient simulation, driven by the same forcings as in the simulation over the period 501–2000, and starting in 1 AD from a quasi-equilibrium simulation corresponding to the forcing estimates for year 1 AD. In order to generate the ensemble of initial simulations required by the data assimilation method, small noise is then added in the atmospheric stream function obtained for years 501 and 601 AD. This perturbation induces a wide spreading of the atmospheric state in the ensemble on a time scale of the order of a few days. The spreading in the ocean is slower but is sufficiently large in year 800 AD when we start the analyses of our experiments (for reasons explained in [Section 2.6](#)).

2.4. Data assimilation method

For the simulations using the particle filter (for more details on the practical implementation, see [Dubinkina et al., 2011](#)), we have chosen to perform an ensemble including 96 members (called particles in the present framework). Previous tests ([Goosse et al., 2006b](#); [Dubinkina et al., 2011](#)) have shown that this provides a good sample of the large-scale variability of the system while being affordable for simulations with data assimilation covering several centuries. Starting from the initial conditions (year 501 AD or 601 AD), each particle is propagated in time by the climate model. After one year, the likelihood of each particle is computed from the difference between the simulated state and the reconstruction at all the locations where reconstructed surface temperatures are available. The particles are then resampled according to their likelihood. The particles with low likelihood are stopped while the particles with a high likelihood are duplicated a number of times proportional to their likelihood. The entire procedure is repeated sequentially every year until the final year of calculations.

The likelihood is based on a Gaussian probability density (as in [van Leeuwen, 2009](#) and in [Dubinkina et al., 2011](#)) using an error covariance matrix which takes into account direct observation errors as well as the error of representativeness (i.e., the fact that models and data are not able to represent the same spatial structures because of grid and sub-grid scale variability present in the data and the lack of observations in some regions to display a true mean on the size of the model grid, e.g., [Kalnay, 2003](#)). We assume that observation errors are uncorrelated and that the error of representativeness is proportional to the covariance between state variables in a long control model run ([Sansó et al., 2008](#)).

2.5. Temperature reconstructions

As mentioned above, two reconstructions are employed here to constrain the model evolution. The [Mann et al. \(2009\)](#) spatial surface temperature reconstructions make use of a global network of more than a thousand proxy records (primarily tree ring, ice core, coral, speleothem, and sediment records) over the past 1500 years. The reconstructions are based on the RegEM climate field reconstruction method ([Mann et al., 2007](#)) which calibrates the proxy network against the spatial information contained within the instrumental annual mean surface temperature over an overlapping (1850–1995) period. This methodology has been thoroughly tested using synthetic proxy networks derived from long-term forced climate model

simulations (Mann et al., 2007). Uncertainties in the reconstructions are estimated from the residual unexplained variance in statistical validation exercises.

The reconstruction of warm season temperatures (April to September temperature) in Europe of Guiot et al. (2010) is based on tree rings, documentaries, pollen and ice cores. The majority of the proxy series (tree-ring and documentary series) have an annual resolution. For a better inference of long-term climate variations, they were completed by a number of low resolution data (decadal or more), mostly of pollen and ice-core data. An original spectral analogue method was devised to deal with this heterogeneous dataset, and especially to preserve the long-term variations and the variability of the temperature series. This reconstruction was validated with a Jack-knife technique, but also by other spatially gridded temperature reconstructions, literature data and glacier advance and retreat curves. Additional tests have been done in Guiot (submitted for publication) to check the robustness of the reconstruction against the uneven spatial coverage of the proxy network in function of time. This has led to the conclusion that the reconstructions were reliable back to A.D. 850.

2.6. Evaluation of the likelihood

The evaluation of the likelihood is performed on spatially smoothed fields in which the features with scales shorter than 4000 km in ASSIM-MANN and 2000 km in ASSIM-GUIOT are efficiently removed. Such a space filtering is required firstly to emphasise the contribution of large-scale structures and secondly to reduce the number of degrees of freedom of the system. Indeed, for systems with many degrees of freedom, a very large number of particles are needed to avoid particle filter degeneracy (for more details see Snyder et al., 2008; van Leeuwen, 2009) while, with the space filtering, it is possible to obtain good results at large scale with a reasonable number of particles. A stronger spatial smoothing is applied in ASSIM-MANN as the selected reconstruction of Mann et al. (2009) covers a much wider area than the one of Guiot et al. (2010). We must insist that the spatial smoothing is applied only in the evaluation of the likelihood and not in any other step of the procedure.

The evaluation of the likelihood is performed every year by comparing the proxy-based reconstructions of annual or summer mean temperatures interpolated on the model grid with the simulated ones at the available data points. For the Mann et al. (2009) reconstruction, the selection of the grid points is restricted to the region northward of 30°N, because our study is focused on extratropical dynamics, while all the data points of the Guiot et al. (2010) reconstruction are kept. The uncertainty of the reconstructions is assumed to be of 0.5 °C for ASSIM-MANN and 0.7 in ASSIM-GUIOT as this is a reasonable estimate of the uncertainty of the reconstructions with the spatial smoothing applied here (Mann et al., 2009; Guiot et al., 2010). However, the results are not very sensitive to such difference in the estimate of the uncertainty. For simplicity, the same uncertainty is applied for every grid point. As the Mann et al. (2009) reconstruction is time filtered using a decadal smoothing filter, a decadal (11-year Butterworth) smoothing filter is applied to the simulation results prior to analysis. We focus (e.g., Fig. 1) on the interval since 800 AD as reconstruction skill is diminished prior that time (Guiot et al., 2010).

3. Results

The mean of the simulations without data assimilation, which provides an estimate of the forced response of the model, shows only a moderate cooling between the Medieval Times and the LIA both in annual mean and in summer at European-scale (Fig. 1). The difference with the reconstructions appears particularly large before 1100 AD, i.e. during the peak of the MCA.

Such moderate temperature changes during the past millennium have also been obtained in a recent simulation performed with a general circulation model driven by a solar forcing characterised by an amplitude similar to the one used here (Jungclaus et al., 2010). When a larger amplitude of the forcing is selected, the temperature changes are also larger (Gonzalez-Rouco et al., 2006; Gosse et al., 2006a; Ammann et al., 2007; Servonnat et al., 2010; Swingedouw et al., 2010). However, although the exact magnitude of past solar irradiance changes is still debated (e.g., Shapiro et al., 2011), the recent recommendations suggest to select a forcing displaying weak variations of TSI as in our experiments (e.g., Gray et al., 2010; Schmidt et al., 2010).

Land use changes play a clear role in the forced response of the model in Europe but it appears a bit smaller than in a previous study with LOVECLIM (Gosse et al., 2006a). This has two main reasons. First, in contrast to the version used in Gosse et al. (2006a), LOVECLIM 1.2 includes a parameterization of the effect of land use on evapotranspiration (Gosse et al., 2010a). Consequently, deforestation reduces the water availability and the evapotranspiration in summer. It induces a surface warming that partly compensates for the albedo effect. Secondly, Gosse et al. (2006a) analysed the whole past millennium. As land-use change is a long-term forcing, characterised by nearly monotonic time development, comparing widely separated periods generally leads to a clearer signal than comparing two closer periods such as the MCA and the LIA.

The data assimilation procedure combines the model results and the proxy-based reconstructions. As a consequence, the simulations with data assimilation are generally between the simulations without data assimilation and the reconstructions. In our experiments, this is associated with simulations with data assimilation presenting lower temperatures during the Medieval Times than the reconstructions in the averages over Europe. However, the simulations ASSIM-MANN and ASSIM-GUIOT still display a clear warm period during Medieval Times, as the reconstruction used to constrain them (Fig. 1).

If we take into account the uncertainty in the reconstructions (Mann et al., 2009; Guiot et al., 2010), the estimate provided by the simulations with data assimilation appears well in the range of the reconstructions. The range of the ensemble of simulations, with thus the internal variability, includes also the reconstructions most of the time. All the estimates based on model simulations and proxies appear thus compatible, at least at the decadal scale used to estimate the uncertainties in Fig. 1. Nevertheless, the persistent high temperatures provided by reconstructions during the MCA still appear to be a quite unlikely state of the model ensemble without data assimilation. The shift induced by data assimilation allows then a closer agreement between the ASSIM-MANN and ASSIM-GUIOT and the reconstructions.

In order to analyse the spatial structure of the changes, we have compared the temperatures in two key periods of the MCA and the LIA (Figs. 2, 3). For the MCA, we have selected the years 900–1050 AD. This may be considered as an early part of the MCA (e.g., Bradley et al., 2003; Mann et al., 2009). However, it roughly corresponds to the maximum temperatures in Europe in the Mann et al. (2009) reconstruction and to high temperatures in the Guiot et al. (2010) reconstruction as well. The latter reconstruction also displays high temperature for the preceding period (800–900) while it shows a temperature decrease at the end of the 11th century. Furthermore, as already mentioned in the Introduction, several proxy records present a cold period after 1050 AD (e.g. Büntgen et al., 2006; Grudd, 2008; Corona et al., 2010). For the LIA, the years 1500–1650 are close to minimal temperatures in both reconstructions. Selecting longer or slightly shifted periods as characteristic of the LIA and the MCA changes our results quantitatively as well as some details of the spatial pattern but does not modify the main conclusions of our study.

The changes obtained in simulations with data assimilation are smoother and have smaller magnitude than the reconstructions

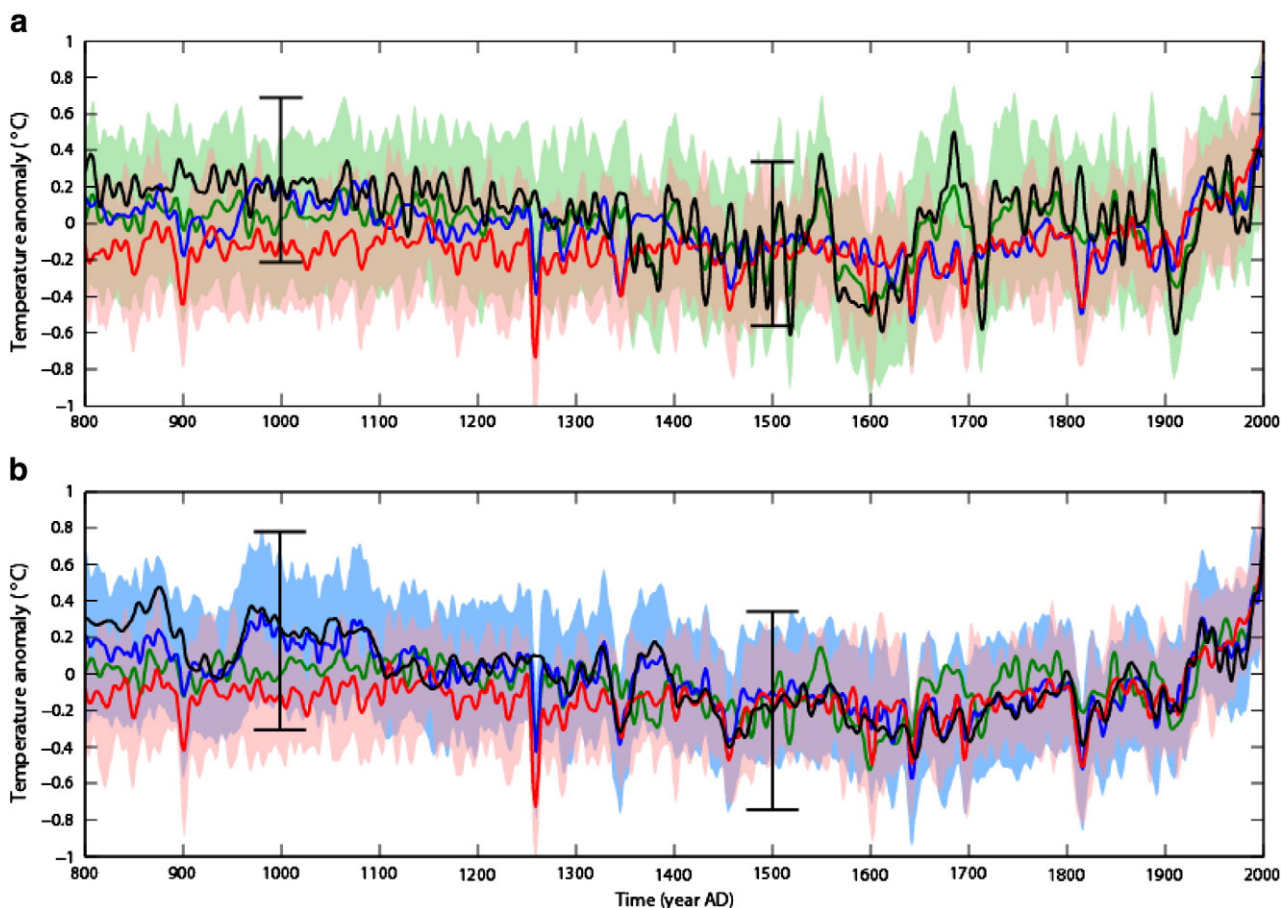


Fig. 1. a) Anomaly of growing season temperature (April to September, °C) averaged over Europe (25°–65°N, 0–60°E) in the reconstruction of Guiot et al. (2010, black), in LOVECLIM simulations without data assimilation (red), in LOVECLIM simulations with data assimilation constrained by Mann et al. (2008) reconstruction (ASSIM-MANN, blue) and in LOVECLIM simulations with data assimilation constrained by Guiot et al. (2010) reconstruction (ASSIM-GUIOT, green). The reference period is 1850–1995. The time series has been filtered using an 11-year running mean. b) Same as a) but for annual mean and the black curve representing the reconstruction of Mann et al. (2008). The pink shading represents the range of the simulations without data assimilation (mean plus and minus two standard deviations), the green shading the one of ASSIM-GREEN (panel a only) and the blue shading the one of ASSIM-MANN (panel b only). The overlap of the uncertainties of the simulations is represented by a darker shading. For the clarity of the plot, the uncertainties of the reconstructions are shown as error bars only for the years 1000 and 1500.

(Fig. 2). This is perfectly consistent with the averages over Europe which have the same characteristics, with the use of coarse resolution model as LOVECLIM and with the spatial smoothing employed in the evaluation of the likelihood in order to emphasise the agreement between model and reconstructions at large-scale. In summer, ASSIM-GUIOT (Fig. 2c) shows maximum temperature differences between the MCA and the LIA in Southern Europe and over the Mediterranean Sea as the Guiot et al. (2010) reconstruction itself (Fig. 2a). The differences between the MCA and the LIA are generally positive in other regions too but their magnitudes are smaller, in particular in Northern and Eastern Europe. Besides, the spatial patterns of the annual mean temperature changes between the MCA and the LIA in the reconstruction of Mann et al. (2009) (Fig. 3a) and in ASSIM-MANN (Fig. 3b) have their maximum at high latitudes. The Mann et al. (2009) reconstruction also displays clearly a minimum difference in Eastern Europe in the latitude band 45–55°N. This is not the case of ASSIM-MANN which has temperatures averaged over Europe in good agreement with Mann et al. (2009) (Fig. 1) but fails in reproducing the detailed spatial structure. ASSIM-MANN basically displays a simple increase in temperature change in a north–east direction as the latitude and the distance to the Atlantic Ocean become higher.

The agreement between the simulations with data assimilation and the reconstruction that is not used to constrain them is much lower. In annual mean, ASSIM-GUIOT (Fig. 3c) still has its maximum over Southern Europe and in Northern Africa and weak changes over

Scandinavia, as in summer. The simulated pattern thus shows little correspondence with that for the Mann et al. (2009) reconstruction. In summer, ASSIM-MANN (Fig. 2b) displays high temperatures at high latitudes but also in South Eastern Europe and Middle East. This is also clearly different from the reconstruction of Guiot et al. (2010). The simulations with data assimilation show thus a much stronger coherency between the summer and annual mean signals than the two reconstructions for the corresponding periods of the year. This may be due to the fact that model that is not able to reconstruct the changes in the right season when driven by annual mean temperatures or to infer the winter (and annual mean) patterns when only summer information is available. On the other hand, with constraints for only one season (or only the annual mean) the most natural solution for the model is likely to give similar changes in all seasons, additional data being required to provide strongly contrasted behaviour during the year.

The response to forcing in annual mean displays a general increase of the changes at high latitudes and in the centre of continents compared to the oceans (Fig. 4). This contributes to explain the changes in ASSIM-MANN at high latitudes in annual mean and in summer. In summer, the forced response at high latitudes is even higher than in ASSIM-GUIOT. The data assimilation is thus damping the changes there. In all the other regions, except in summer at mid-latitude around 70°E, the forced signal is much weaker than the one seen in the simulations with data assimilation. In particular, the

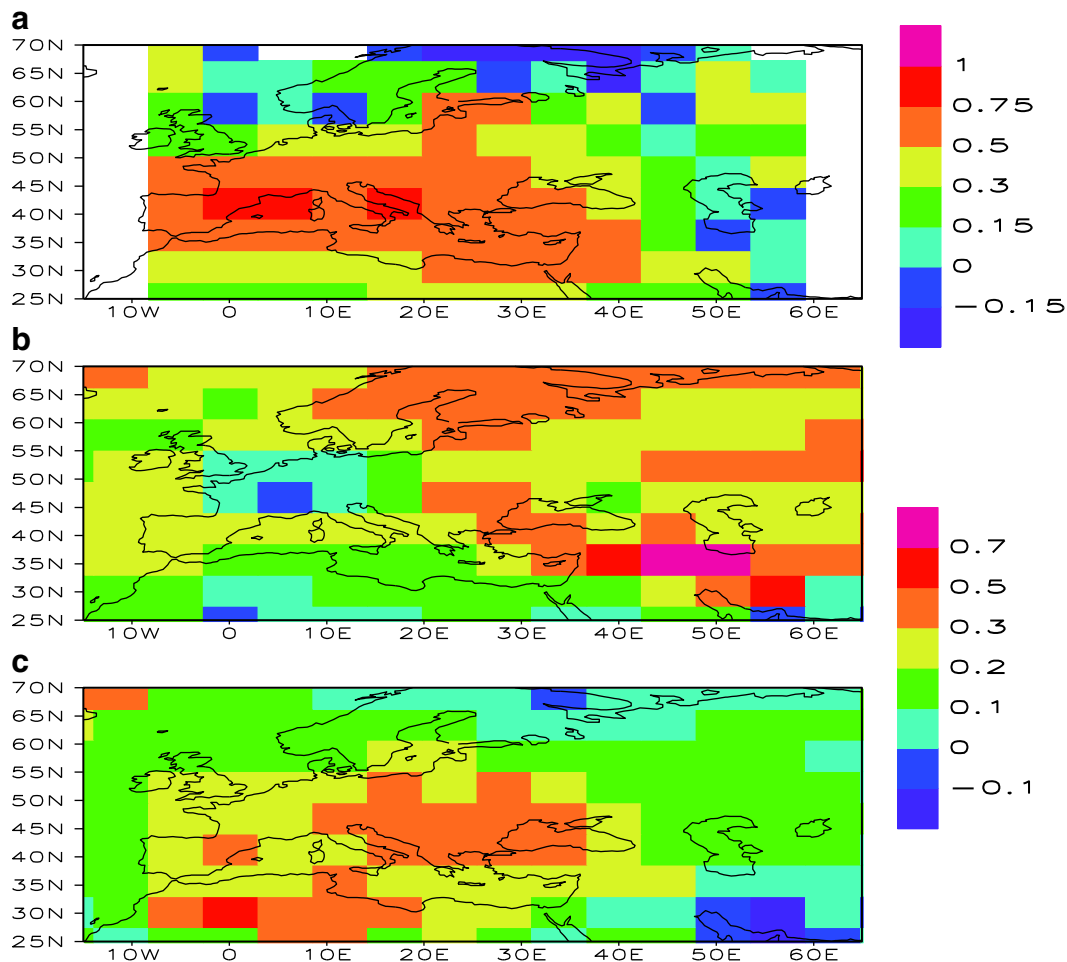


Fig. 2. Difference in growing season surface temperature (April to September, °C) between key periods of the MCA (900–1050) and the LIA (1500–1650) a) in the reconstruction of Guiot et al. (2010), b) in ASSIM-MANN, and c) in ASSIM-GUIOT. Pay attention that a different colour code is employed for the reconstruction and the simulations to emphasise the spatial structure of the changes.

summer changes in Western Europe at about 50°N are very weak between the LIA and the MCA in simulations without data assimilation: the warming during the LIA associated with the reduced evapotranspiration caused by deforestation compensates for the warming effect of the other forcings in the model.

If the major fraction of the simulated changes in ASSIM-GUIOT and ASSIM-MANN cannot be explained by the forced response of the model, they must find their origin in the circulation simulated in those experiments. In annual mean, the difference in atmospheric circulation over Europe between the MCA and the LIA in MANN-ASSIM has strong similarities with the positive phase of the NAO. It displays positive anomalies of geopotential height at around 40°N over the East Atlantic and negative ones around Iceland (Fig. 5a). This is mainly resulting from a winter signal, the summer pattern being quite different (Fig. 6a). The associated increase in the westerlies over the Atlantic and Northern Europe implies a warming in MANN-ASSIM at high latitudes in winter, contributing thus to the annual mean signal displayed in Fig. 3b. This positive winter NAO phase can also lead to summer warming, as the winter NAO has an impact on the sea surface temperature that can induce temperature anomalies in the following seasons (e.g., van der Schrier and Barkmeijer, 2005).

The annual mean circulation changes in ASSIM-GUIOT are quite different (Fig. 5b), showing negative anomalies centred over Portugal and Morocco and positive ones between Iceland and Norway. In this experiment, the annual mean circulation anomaly appears mainly as a reminiscent of the summer signal driven by the assimilation, the

changes in winter being relatively small. It induces a reduction of the summer westerlies in Western Europe and southerly winds in central Mediterranean that bring warm air to the Mediterranean Sea and Europe.

The summer signal in ASSIM-MANN has some similarities with the one of ASSIM-GUIOT: the geopotential height is lower over the North Atlantic at mid latitudes and is higher in the Northeast Atlantic during the MCA (Fig. 6a). However, some clear differences are also present. The most important one is likely the smaller extent of the negative anomalies that are restricted to the North Atlantic in ASSIM-MANN while they cover also the Iberian Peninsula in ASSIM-GUIOT. This has a large impact on the simulated temperatures since the southerly winds over the central Mediterranean that warm up Southern Europe in ASSIM-GUIOT are absent in ASSIM-MANN. An interpretation of this difference is that the additional information in summer used in ASSIM-GUIOT compared to ASSIM-MANN is sufficient to induce modest changes in the circulation itself (Fig. 6) that have a large impact on the temperature pattern (Fig. 2).

Changes in winter circulation (and consequently in annual mean) in ASSIM-MANN and the associated temperature changes in Northern Europe appear quite classical for the NAO (e.g. Hurrell, 1995; Wanner et al., 2001) and such a positive NAO signal during medieval times has been proposed in many previous studies (e.g., Shindell et al., 2003; Mann et al., 2009; Trouet et al., 2009; Graham et al., 2010). In contrast to the winter, the season when the atmosphere is the most active, the circulation in summer and its impact on European temperatures have been the subject to much less studies, both for the present conditions

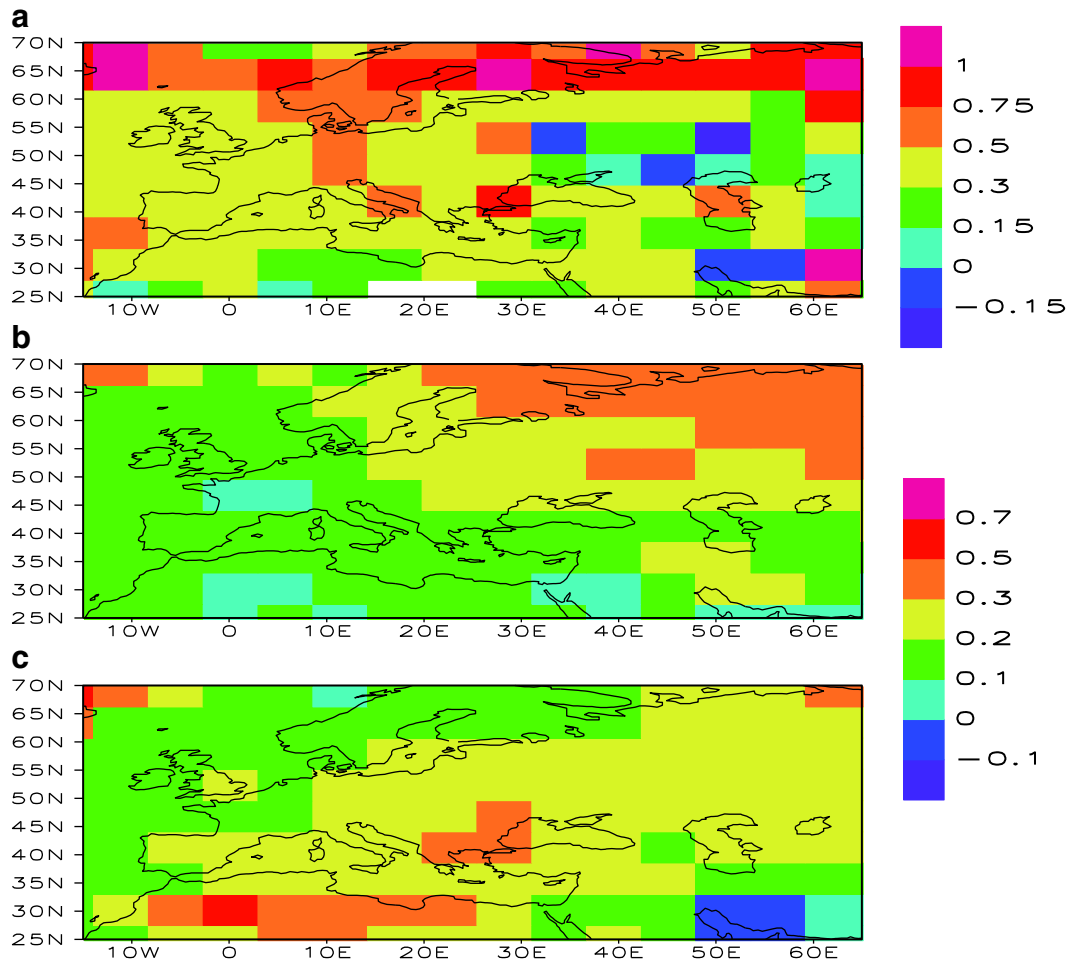


Fig. 3. Difference in annual mean surface temperature ($^{\circ}\text{C}$) between key periods of the MCA (900–1050) and the LIA (1500–1650) a) in the reconstruction of Mann et al. (2008), b) in ASSIM-MANN, and c) in ASSIM-GUIOT. Pay attention that a different colour code is employed for the reconstruction and the simulations to emphasise the spatial structure of the changes.

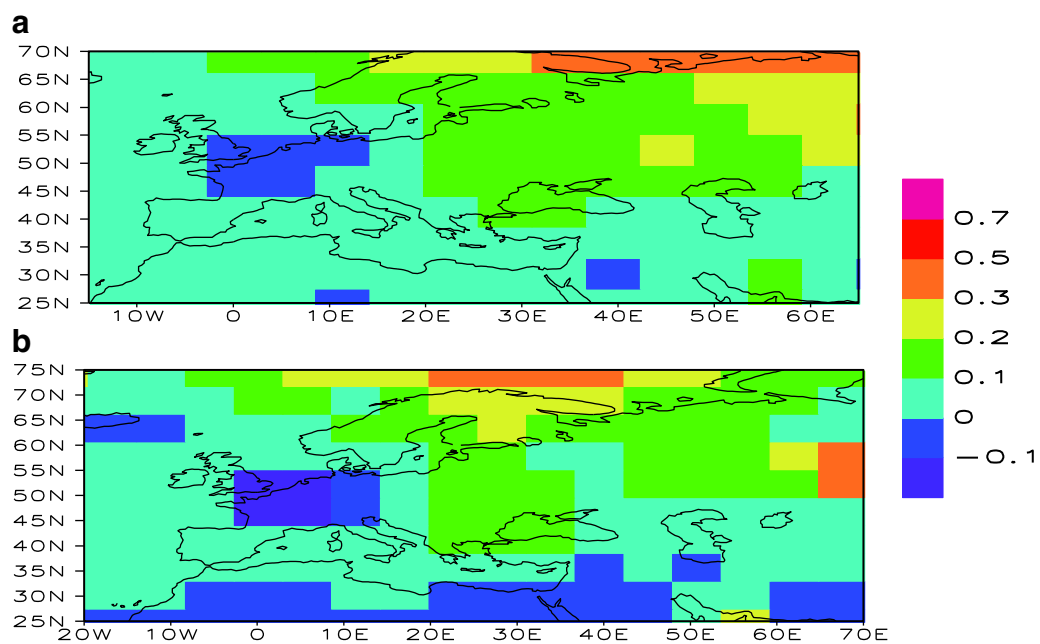


Fig. 4. Difference in surface temperature ($^{\circ}\text{C}$) between key periods of the MCA (900–1050) and the LIA (1500–1650) in simulation without data assimilation a) in annual mean and b) in summer.

to an opposite trend of the SNAO. However, the link between sea surface temperature and pressure in the western Atlantic does not seem to be robust in all the models and additional work is required to confirm or not this link (e.g. Hodson et al., 2010).

The circulation simulated for the MCA compared to the LIA in summer (Fig. 6) also displays modified westerlies and thus changes in the transport of moist and relatively cold Atlantic water masses towards Europe as in the SNAO. However, although the centres of action in the model are also shifted northward compared to winter patterns, the shift is much smaller in the model than in the observed SNAO. As a consequence, the change in the polarity of the anomalies

occurs much southward in Fig. 6 than in the SNAO pattern of Folland et al. (2009). The simulated difference between the MCA and the LIA could thus not be reasonably interpreted as simply as a change in the probability of the SNAO phases in our experiments.

An alternative method to those analyses centred on the dominant mode of variability of the atmospheric circulation is to study the circulation patterns associated with warm conditions in Europe. Over the past 150 years, high summer temperatures in Central and Southern Europe are observed when sea level pressure is high there and when the pressure is lower than normal over the Atlantic (Fig. 7a). This link between high pressure and high summer

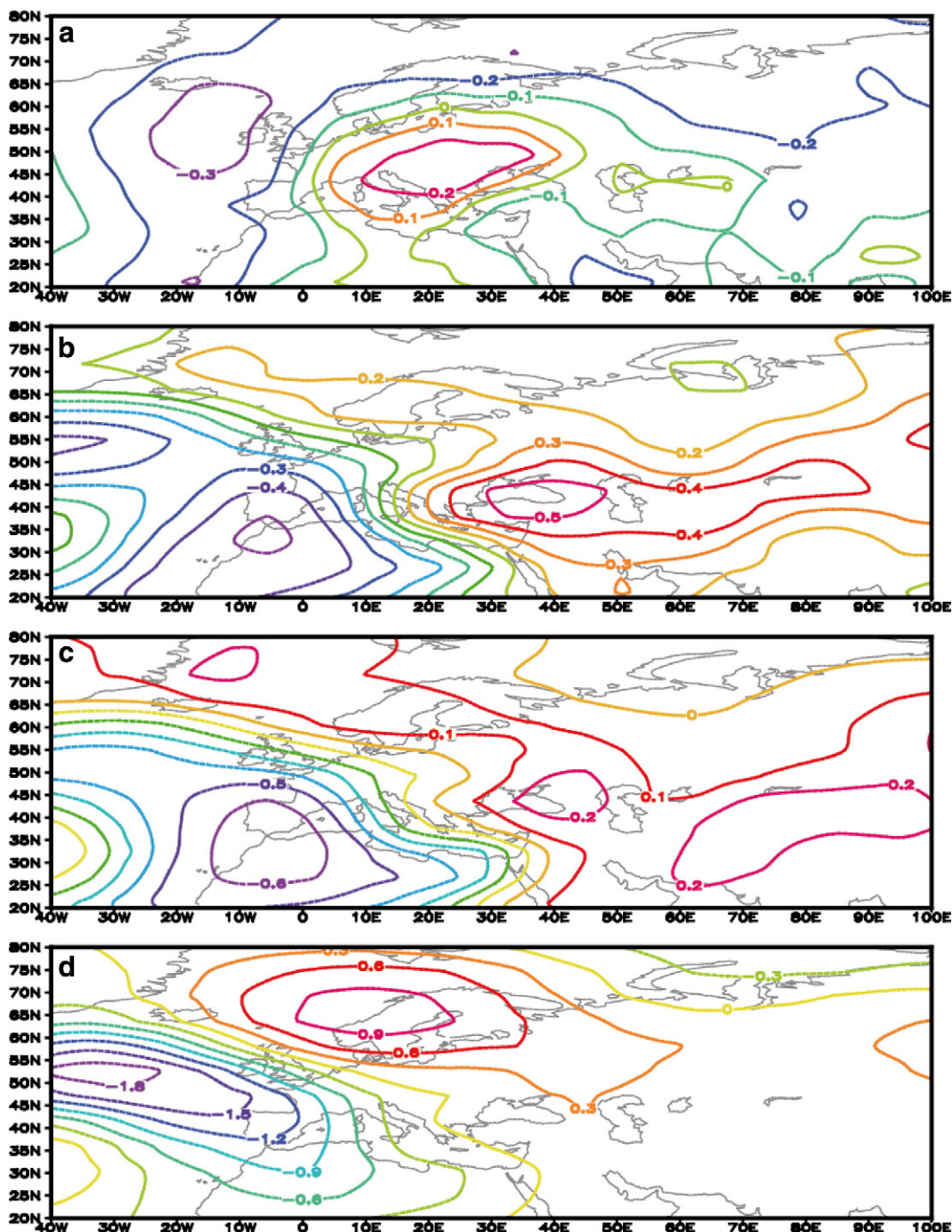


Fig. 7. a) Correlation between sea level pressure (HADSLP2 data set, Allan and Ansell, 2006) and growing season temperature (HADCRUT3 dataset, Brohan et al., 2006) in Southern Europe (0–20°E, 35–50°N) for the period 1850–2000. b) Correlation between geopotential height at 800 hpa and growing season temperature in Southern Europe (0–20°E, 35–50°N) in ASSIM-GUIOT for the period 1850–2000 and c) for the period 600–2000. d) Regression (in m) between geopotential height at 800 hpa and growing season temperature in Southern Europe (0–20°E, 35–50°N) in ASSIM-GUIOT for the period the period 600–2000.

temperature is classical for many European regions and has been discussed in several studies (e.g. [Jacobeit et al., 2002](#); [Gouriand et al., 2007](#); [Folland et al., 2009](#)). This link is also found in ASSIM-GUIOT. For the last 150 years, the correlations between geopotential height and temperature in this experiment reproduce many characteristics of the corresponding values for observations although the correlations are higher and the spatial extent of the positive values over Europe is larger ([Fig. 7b](#)). When the whole length of ASSIM-GUIOT is analysed, the correlations decrease but the spatial structure remains the same ([Fig. 7c](#)). The pattern obtained from correlation and regression analysis ([Fig. 7cd](#)) is different from [Fig. 6b](#) as expected, the period of interest and the diagnostic being different. However, both [Fig. 6b](#) and all the panels of [Fig. 7](#) are characterised by opposite changes over Europe and North Atlantic at low and mid-latitudes, inducing Southerly winds over the Western Europe and Mediterranean Sea. This confirms the potential role of these circulation changes in the warming observed there during the MCA.

4. Discussion

The results analysed in the previous section have shown that it is possible to constrain LOVECLIM to follow the signal recorded in the two proxy-based reconstructions using a particle filter with an ensemble size of the order of 100 and to derive from our simulations some insight in the mechanisms responsible for the temperature changes during the MCA. Our experimental design is valid to reach the goals defined in the introduction, but some of our conclusions are influenced by the choices performed. Two, partly related, key elements need to be discussed here in some extent: first the nature of the spatial and seasonal structures of the changes during the MCA and second the role of the external forcing in the observed changes.

Although the reconstructions of [Mann et al. \(2009\)](#) and [Guiot et al. \(2010\)](#) both display a clear and strong MCA in Europe, their spatial patterns are clearly different: in annual mean, the [Mann et al. \(2009\)](#) reconstruction has its maximum at high latitudes, while the highest summer temperature changes in summer are found in Southern Europe in [Guiot et al. \(2010\)](#). The simulations with data assimilation are in good agreement with the reconstruction that is used to constrain them, showing that the reconstructed patterns based on proxy records are perfectly consistent with the model physics. However, the model results suggest only a weak link between the seasons. When driven by annual mean temperatures in ASSIM-MANN, only a few characteristics of the summer climate obtained in ASSIM-GUIOT, such as the reduced westerlies, can be reproduced. In this latter experiment, the constraints imposed in summer have a weak impact in winter.

A hypothesis is that the two seasons are only weakly coupled. However, it seems unlikely that warm conditions during both summer and winter would occur for entirely unrelated reasons. An alternative hypothesis is that the observed changes in Europe in both seasons are related to a common factor that is not accounted for in our experiments. Temperature changes over the North Atlantic are obviously one candidate, but the exact impact of temperature anomalies over the Atlantic on European climate is still not precisely known (e.g. [Hodson et al., 2010](#)). [Graham et al. \(2010\)](#) have recently argued that many characteristics of the MCA can be explained as the response of the system to warm conditions in the tropical Indian and western Pacific Oceans. Their study fails to reproduce a summer warming in Europe, but combining their hypothesis with a warm North Atlantic, for instance, could explain the reconstructed climate changes in Europe. In our experiments, there are no data assimilation constraints applied in the tropics. The tropical–extra tropical interactions are not well represented in ECBILT ([Opsteegh et al., 1998](#)) precluding any investigation of the exact role of those interactions. Such connections could be investigated by simulations with comprehensive General Circulation Models or potentially through the

inclusion of some of missing tropical ocean–atmosphere physics within LOVECLIM itself—a subject of current investigation.

Like the models, the reconstructions themselves may contain biases. Both reconstructions used in this study have demonstrated skill at the scale of the European continent ([Mann et al., 2009](#); [Guiot et al., 2010](#)). That finding is consistent with the notion that climate field reconstruction methods yield greatest skill in regions such as Europe where data density is high ([Smerdon et al., 2011](#)). Uncertainties in either or both reconstruction may nonetheless explain some of the features that we have interpreted so far as, for instance, differences in seasonal representativeness. While [Mann et al. \(2009\)](#) reconstruct annual mean temperature, the various underlying proxy records often have seasonally-specific sensitivity, particularly in the mid-latitudes where considerable use is made of tree-ring records which may alternatively reflect either e.g. warm-season temperatures or cold-season precipitation, depending on the environment from which they come. At the regional scale of e.g. Europe, it is thus possible that the distribution of proxy records preferentially biases the seasonality represented by the reconstruction. Additionally, the features inferred in the two reconstructions are not necessarily consistent with all available proxy evidence. For instance, the [Guiot et al. \(2010\)](#) reconstruction displays relatively mild conditions in Scandinavia during Medieval times while there is no indication of a warm period seen around 1000–1050 in some proxies from the region (e.g., [Briffa et al., 1992](#); [Grudd, 2008](#)). For the more recent past, the comparison of the [Guiot et al. \(2010\)](#) reconstructions with that of [Luterbacher et al. \(2004\)](#) and [Casty et al. \(2007\)](#) shows reasonably good concordance over certain periods but a lack of correspondence during others (see [Guiot et al., 2010](#) for more details). The local features in the reconstructions selected here must thus be interpreted with caution but previous validation tests suggest that for the larger-scale features of interest in this study, the information in the reconstructions is reasonably reliable and robust.

The methods used by [Mann et al. \(2009\)](#) and [Guiot et al. \(2010\)](#) are different in terms of the underlying assumptions. The former employs a covariance-based climate field reconstruction approach, while the latter uses an analogue-based spatial pattern matching approach. The analogue approach may suffer if sufficient analogues to modern patterns of variability do not apply to the past. The covariance-based approach, on the other hand, is limited by the relatively few statistical degrees of freedom retained in the data, particularly in earlier centuries—something that becomes increasingly problematic when focusing on relatively small spatial regions such as Europe (see discussion in [Mann et al., 2009](#)). Despite the fact that they share some proxies (in particular some tree rings data), the limitations of these two methods, and associated potential biases, are arguably different, potentially explaining the divergence between the ASSIM-MANN and ASSIM-GUIOT results.

The response to the forcing is relatively weak in LOVECLIM and contributes only to a small fraction of the changes obtained in the simulations with data assimilation, except in some regions. However, this response may be underestimated because of uncertainties in the reconstruction of the forcing or because of missing physics in LOVECLIM. In particular, the model does not have interactive clouds than can play a crucial role in amplifying the temperature changes over Europe in summer. It also fails in reproducing a strong enough response of the atmospheric circulation to volcanic eruption or changes in solar irradiance ([Goosse and Renssen, 2004](#)). Furthermore, we impose relatively weak changes in solar irradiance while some reconstructions suggest larger ones (e.g. [Shapiro et al., 2011](#)).

An argument in favour of the underestimation of the role of the forcing in our experiment is the systematically lower temperatures during the MCA in the simulations with data assimilation compared to the reconstructions. However, this difference between the simulations with data assimilation and the reconstructions can also be seen as a characteristic of the technique itself that looks for a

compromise between on the one hand the forcing and model physics (weak systematic signal) and on the other hand the reconstructions (large signal). Furthermore, general circulation models, driven by various estimates of the forcings, also fail in reproducing well the reconstructed temperature changes in Europe (e.g., Gómez-Navarro et al., 2010; Servonnat, 2011). This indicates, at least, that the forcing may not be responsible alone for the spatial structure of the changes in our experiments. Finally, the spatial pattern of the response to the forcing and the one of the reconstructions is quite different. Increasing the amplitude of the solar forcing for instance would contribute to a larger response at high latitudes. However, it would not reduce the disagreement at regional scale, in particular in summer when the maximum temperature changes during the MCA are observed in Southern Europe in Guiot et al. (2010). This latter argument is probably not valid for the potential impact of a different response to land-use changes, related to improved model physics or the choice of a different reconstruction, as this response has a spatial structure that strongly depends on the regional distribution of the imposed changes and on the model itself.

In summary, we can state that our interpretation of the simulations with data assimilation appears valid using the present knowledge of the system and that there is no strong reason to consider that any of the choice we have made in the experimental design has led to major biases in our results. However, it would be worthwhile to ensure that we have not underestimated some sources of uncertainties. In particular, we have assumed, in agreement with previous analyses, that a majority of the differences between Mann et al. (2009) and Guiot et al. (2010) were related to the different target season, not to differences in the methodology. However, a comprehensive assessment of the role of the methodology would help further validate (or reject) this hypothesis, allowing for further refinement of our conclusions. Determining the exact role of forcing changes will require more precise forcing scenario and additional simulations with state-of-the-art models analysing in details the mechanisms responsible for the response of the climate system. We have underlined the role of atmospheric circulation anomaly in past change. For both seasons, the patterns could be justified using simple physical arguments and appears robust. However, in our simulation with data assimilation, circulation changes have their origin in the internal variability of the system. Alternatively, they could also be the manifestation of the response of the system to external forcing or to remote changes through mechanisms not well taken into account in our experiments.

5. Conclusions

Using two different temperature reconstructions employing a variety of individual climate proxy records, and assimilating those reconstructions into a climate model of intermediate complexity, we have characterised the seasonal and spatial features of temperature changes in Europe during the MCA. Moreover, using the dynamical consistency insured by the model/data synthesis framework, we are able to propose specific hypotheses regarding the large-scale atmospheric circulation anomalies most consistent with those changes. We thus consider the study to represent a successful application of data assimilation to the problem of interpreting climate changes of the past millennium.

Other past work has explored the complex spatio-temporal structure of the transition between the MCA and the LIA (e.g. Hughes and Diaz, 1994; Bradley et al., 2003; Mann et al., 2009). In the current study, we find that even at the continental scale of Europe, the MCA displays a rich structure that cannot be characterised as an anomaly that is uniformly warm in space and time, a finding that is consistent with analyses of the past several centuries (e.g. Luterbacher et al., 2004) but which extends this conclusion further back through the MCA interval. Perhaps most significantly, our data assimilation

approach provides a potentially deeper understanding of the atmospheric dynamics that can explain the observed spatial structure to the European MCA temperature patterns.

In our simulations with data assimilation, warm MCA conditions at high latitude can be explained by a combination of positive radiative forcing and a winter circulation anomaly with similarities to the positive phase of the NAO, that is associated with enhanced advection of warm maritime into the continent. In summer, as the Atlantic Ocean is colder than the neighbouring European continent, warm MCA conditions are instead associated with reduced westerlies over Western Europe. The substantial summer warming in Southern Europe and the Mediterranean Sea displayed by the Guiot et al. (2010) reconstruction can be interpreted in the context of anomalous advection of warm air from North Africa. Owing to the limited representation of tropical/extratropical climate linkages in the climate model used, our study cannot establish whether the observed changes are a consequence of local dynamics, a response to remote forcing from e.g. the tropical oceans, or some complex dynamical response to changes in radiative forcing. Distinguishing between such alternative possible explanations of the inferred regional climate changes, and gaining a deeper understanding of the climate dynamics underlying the MCA and other anomalous climate intervals in Europe represent a major thrust of our efforts to build upon the current data assimilation framework.

Acknowledgements

H. Goosse is Research Associate with the Fonds National de la Recherche Scientifique (F.R.S.-FNRS-Belgium). This work is supported by the F.R.S.-FNRS and by the Belgian Federal Science Policy Office (Research Program on Science for a Sustainable Development) and by EU (project Past4future). M.E. Mann gratefully acknowledges support from the NSF Paleoclimate program (grant number ATM-0902133). J. Guiot acknowledges support from the French National Research Agency (program VMC, project ESCARSEL ANR-06-VULN-010). Aurélien Mairesse helped in the design of Fig. 1. The simulations were performed on the computers of the Institut de calcul intensif et de stockage de masse of the Université catholique de Louvain.

References

- Allan, R., Ansell, T., 2006. A new globally complete monthly historical gridded mean sea level pressure dataset (HadSLP2): 1850–2004. *J. Clim.* 19, 5816–5842.
- Ammann, C.M., Joos, F., Schimel, D.S., Otto-Bliesner, B.L., Tomas, R.A., 2007. Solar influence on climate during the past millennium: results from transient simulations with the NCAR Climate System Model. *Proc. Natl. Acad. Sci. U. S. A.* 104, 3713–3718.
- Bard, E., Raisbeck, G., Yiou, F., Jouzel, J., 2000. Solar irradiance during the last 1200 years based on cosmogenic nuclides. *Tellus* 52B, 985–992.
- Barnston, A.G., Livezey, R.E., 1987. Classification, seasonality and persistence of low-frequency atmospheric circulation patterns. *Mon. Weather Rev.* 115, 1083–1126.
- Bengtsson, L., Hodges, K.L., Roeckner, E., Brokopf, R., 2006. On the natural variability of the pre-industrial European climate. *Clim. Dyn.* 27, 743–760.
- Berger, A.L., 1978. Long-term variations of daily insolation and quaternary climatic changes. *J. Atmos. Sci.* 35, 2363–2367.
- Bradley, R.S., Hughes, M.K., Diaz, H.F., 2003. Climate in Medieval time. *Science* 302, 404–405.
- Brewer, S., Alleaume, S., Guiot, J., Nicault, A., 2006. Historical droughts in Mediterranean regions during the last 500 years: a data/model approach. *Clim. Past* 3, 355–366.
- Briffa, K.R., Jones, P.D., Bartholin, T.S., Eckstein, D., Schweingruber, F.H., Karlén, W., Zetterberg, P., Eronen, M., 1992. Fennoscandian summers from AD 500: temperature changes on short and long timescales. *Clim. Dyn.* 7, 111–119.
- Brohan, P., Kennedy, J.J., Harris, I., Tett, S.F.B., Jones, P.D., 2006. Uncertainty estimates in regional and global observed temperature changes: a new data set from 1850. *J. Geophys. Res.* 111, D12106 doi:10.1029/2005JD006548.
- Brovkin, V., Bendtsen, J., Claussen, M., Ganopolski, A., Kubatzki, C., Petoukhov, V., Andreev, A., 2002. Carbon cycle, vegetation and climate dynamics in the Holocene: experiments with the CLIMBER-2 model. *Glob. Biogeochem. Cycles* 16. doi:10.1029/2001GB001662.
- Brovkin, V., Claussen, M., Driesschaert, E., Fichetef, T., Kicklighter, T., Loutre, M.-F., Matthews, H.D., Ramankutty, N., Schaeffer, M., Sokolov, A., 2006. Biogeophysical effects of historical land cover changes simulated by six Earth system models of intermediate complexity. *Clim. Dyn.* 26 (6), 587–600.

- Büntgen, U., Esper, J., Frank, D.C., Nicolussi, K., Schmidhalter, M., 2005. A 1052-year tree-ring proxy for Alpine summer temperatures. *Clim. Dyn.* 25, 141–153.
- Büntgen, U., Frank, D.C., Nievergelt, D., Esper, J., 2006. Summer temperature variations in the European Alps, A.D. 755–2004. *J. Clim.* 19, 5607–5623.
- Casty, C., Raible, C.C., Stocker, T.F., Wanner, H., Luterbacher, J., 2007. A European pattern climatology 1766–2000. *Clim. Dyn.* 29, 791–805.
- Charlson, R.J., Langner, J., Rodhe, H., Leovy, C.B., Warren, S.G., 1991. Perturbation of the Northern Hemisphere radiative balance by backscattering from anthropogenic sulfate aerosols. *Tellus* 43 AB, 152–163.
- Charman, D.J., 2010. Centennial climate variability in the British Isles during the mid-late Holocene. *Quatern. Sci. Rev.* 29, 1539–1554.
- Corona, C., Guiot, J., Edouard, J.L., Chalié, F., Büntgen, U., Nola, P., Urbinati, C., 2010. Millennium-long summer temperature variations in the European Alps as reconstructed from tree rings. *Clim. Past* 6, 379–400.
- Crespin, E., Goosse, H., Fichet, T., Mann, M.E., 2009. The 15th century Arctic warming in coupled model simulations with data assimilation. *Clim. Past* 5, 389–401.
- Crowley, T.J., Baum, S.K., Kim, K.Y., Hegerl, G.C., Hyde, W.T., 2003. Modeling ocean heat content changes during the last millennium. *Geophys. Res. Lett.* 30, 1932.
- Delaygue, G., Bard, E., 2010. An Antarctic view of Beryllium-10 and solar activity for the past millennium. *Clim. Dyn.* 36, 2201–2218. doi:10.1007/s00382-010-0795-1.
- Dubinkina, S., Goosse, H., Sallaz-Damaz, Y., Crespin, E., Crucifix, M., 2011. Testing a particle filter to reconstruct climate changes over the past centuries. *Int. J. Bifurc. Chaos* 13, 2011–6106.
- Feddema, J., Oleson, K., Bonan, G., Mearns, L., Washington, W., Meehl, G., Nychka, D., 2005. A comparison of a GCM response to historical anthropogenic land cover change and model sensitivity to uncertainty in present-day land cover representation. *Clim. Dyn.* 25, 581–609.
- Fischer, E.M., Luterbacher, J., Zorita, E., Tett, S.F.B., Casty, C., Wanner, H., 2007. European climate response to tropical volcanic eruptions over the last half millennium. *Geophys. Res. Lett.* 34, L05707. doi:10.1029/2006GL027992.
- Folland, C.K., Knight, J., Linderholm, H.W., Fereday, D., Ineson, S., Hurrell, J.W., 2009. The summer North Atlantic Oscillation. *J. Clim.* 22, 1082–1103.
- Foukal, P., Fröhlich, C., Spruit, H., Wigley, T.M.L., 2006. Variations in solar luminosity and their effect on the Earth's climate. *Nature* 443, 161–166.
- Gaillard, M.-J., Sugita, S., Mazier, F., Trondman, A.-K., Broström, A., Hickler, T., Kaplan, J.O., Kjellström, E., Kokfelt, U., Kuneš, P., Lemmen, C., Miller, P., Olofsson, J., Poska, A., Rundgren, M., Smith, B., Strandberg, G., Fyfe, R., Nielsen, A.B., Alenius, T., Balakauskas, L., Barnekow, L., Birks, H.J.B., Bjune, A., Björkman, L., Giesecke, T., Hjelte, K., Kalnina, L., Kangur, M., van der Knaap, W.O., Koff, T., Lagerås, P., Latalowa, M., Leydet, M., Lechterbeck, J., Lindbladh, M., Odogaard, B., Peglar, S., Segerström, U., von Stedingk, H., Seppä, H., 2010. Holocene land-cover reconstructions for studies on land cover-climate feedbacks. *Clim. Past* 6, 483–499.
- Gao, C.C., Robock, A., Ammann, C., 2008. Volcanic forcing of climate over the past 1500 years: an improved ice core-based index for climate models. *J. Geophys. Res.* 113, D23111. doi:10.1029/2008JD012339, 2008.
- Gómez-Navarro, J.J., Montávez, J.P., Jerez, S., Jiménez-Guerrero, P., Lorente-Plazas, R., González-Rouco, J.F., Zorita, E., 2010. A regional climate simulation over the Iberian Peninsula for the last millennium. *Clim. Past Discuss.* 6, 2071–2116.
- Gonzalez-Rouco, J.F., Beltrami, H., Zorita, E., von Storch, H., 2006. Simulation and inversion of borehole temperature profiles in surrogate climates: spatial distribution and surface coupling. *Geophys. Res. Lett.* 33, L01703. doi:10.1029/2005GL024693.
- Goosse, H., Fichet, T., 1999. Importance of ice-ocean interactions for the global ocean circulation: a model study. *J. Geophys. Res.* 104, 23337–23355.
- Goosse, H., Renssen, H., 2004. Exciting natural modes of variability by solar and volcanic forcing: idealized and realistic experiments. *Clim. Dyn.* 23, 153–163.
- Goosse, H., Renssen, H., Timmermann, A., Bradley, R.S., 2005. Internal and forced climate variability during the last millennium: a model-data comparison using ensemble simulations. *Quatern. Sci. Rev.* 24, 1345–1360.
- Goosse, H., Arzel, O., Luterbacher, J., Mann, M.E., Renssen, H., Riedwyl, N., Timmermann, A., Xoplaki, E., Wanner, H., 2006a. The origin of the European “Medieval Warm Period”. *Clim. Past* 2, 99–113.
- Goosse, H., Renssen, H., Timmermann, A., Bradley, R.S., Mann, M.E., 2006b. Using paleoclimate proxy-data to select optimal realisations in an ensemble of simulations of the climate of the past millennium. *Clim. Dyn.* 27, 165–184. doi:10.1007/s00382-006-0128-6.
- Goosse, H., Brovkin, V., Fichet, T., Haarsma, R., Jongma, J., Huybrechts, P., Mouchet, A., Seltén, F., Barriat, P.-Y., Campin, J.-M., Deleersnijder, E., Driesschaert, E., Goelzer, H., Janssens, I., Loutre, M.-F., Morales Maqueda, M.A., Opsteegh, T., Mathieu, P.-P., Munhoven, G., Petterson, E., Renssen, H., Roche, D.M., Schaeffer, M., Severijns, C., Tartinville, B., Timmermann, A., Weber, N., 2010a. Description of the Earth system model of intermediate complexity LOVECLIM version 1.2. *Geosci. Mod. Dev.* 3, 603–633.
- Goosse, H., Crespin, E., de Montety, A., Mann, M.E., Renssen, H., Timmermann, A., 2010b. Reconstructing surface temperature changes over the past 600 years using climate model simulations with data assimilation. *J. Geophys. Res.* 115, D09108. doi:10.1029/2009JD012737.
- Goudie, A., 1993. *The Human Impact on the Natural Environment*, fourth edition. Blackwell Publishers, Oxford, UK. 454 pages.
- Gouriland, I., Moberg, A., Zorita, E., 2007. Climate variability in Scandinavia for the past millennium simulated by an atmosphere-ocean general circulation model. *Tellus* 59A, 30–49.
- Graham, N.E., Ammann, C.M., Fleitmann, D., Cobb, K.M., Luterbacher, J., 2010. Support for global climate reorganization during the ‘Medieval Climate Anomaly’. *Clim. Dyn.* doi:10.1007/s00382-010-0914-z
- Gray, L.J., Beer, J., Geller, M., Haigh, J.D., Lockwood, M., Matthes, K., Cubash, U., Fleitmann, D., Harrison, G., Hood, L., Luterbacher, J., Meehl, G.A., Shindell, D., van Geel, B., White, W., 2010. Solar influences on climate. *Rev. Geophys.* 48, RG4001. doi:10.1029/2009RG000282.
- Grudh, H., 2008. Torneträsk tree-ring width and density ad 500–2004: a test of climatic sensitivity and a new 1500-year reconstruction of north Fennoscandian summers. *Clim. Dyn.* 31, 843–857.
- Guiot, J., submitted for publication. A robust spatial reconstruction of April to September temperature in Europe: comparisons between the Medieval Period and the recent warming with a focus on extremes values. *Global Planetary Change*.
- Guiot, J., Corona, C., ESCARSEL members, 2010. Growing season temperatures in Europe and climate forcings over the past 1400 years. *PLOS One* 5 (4), 1–15.
- Gunnarson, B., Linderholm, H.W., Modberg, A., 2010. Improving a tree-ring reconstruction from west-central Scandinavia: 900 years of warm-season temperatures. *Clim. Dyn.* doi:10.1007/s00382-010-0783-5.
- Hegerl, G.C., Crowley, T.J., Allen, M., Hyde, W.T., Pollack, H.N., Smerdon, J., Zorita, E., 2007. Detection of human influence on a new, validated 1500-year temperature reconstruction. *J. Clim.* 20, 650–666.
- Hegerl, G., Luterbacher, J., González-Rouco, F., Tett, S.F.B., Crowley, T., Xoplaki, E., 2011. Influence of human and natural forcing on European seasonal temperatures. *Nat. Geosci.* 4, 99–103.
- Hiller, A., Boettger, T., Kremenetski, C., 2001. Medieval climate warming recorded by radiocarbon dated alpine tree-line shift on the Kola Peninsula, Russia. *Holocene* 11, 491–497.
- Hodson, D.L.R., Sutton, R.T., Cassou, C., Keenlyside, N., Okumura, Y., Zhou, T.J., 2010. Climate impacts of recent multidecadal changes in Atlantic Ocean Sea Surface Temperature: a multimodel comparison. *Clim. Dyn.* 34, 1041–1058.
- Hughes, M.K., Diaz, H.F., 1994. Was there a “Medieval Warm Period”, and if so, where and when? *Climate Change* 26, 109–142.
- Hurrell, J.W., 1995. Decadal trends in the North Atlantic oscillation: regional temperatures and precipitation. *Science* 269, 676–679.
- Jacobbeit, J., Wanner, H., Luterbacher, J., Beck, C., Philipp, A., Sturm, K., 2002. Atmospheric circulation variability in the North-Atlantic-European area since the mid-seventeenth century. *Clim. Dyn.* 20 (4), 341–352.
- Jansen, E., Overpeck, J., Briffa, K.R., Duplessy, J.-C., Joos, F., Masson-Delmotte, V., Olago, D., Otto-Bliesner, B., Peltier, W.R., Rahmstorf, S., Ramesh, R., Raynaud, D., Rind, D., Solomina, O., Villalba, R., Zhang, D., 2007. Palaeoclimate. In: Solomon, S., Qin, D., Manning, M., Chen, Z., Marquis, M., Averyt, K.B., Tignor, M., Miller, H.L. (Eds.), *Climate Change 2007: The Physical Science Basis*. Contribution of Working Group I to the Fourth Assessment Report of the Intergovernmental Panel on Climate Change. Cambridge University Press, Cambridge, United Kingdom and New York, NY, USA.
- Jiang, H., Eiriksson, J., Schulz, M., Knudsen, K.L., Seidenskrantz, M.-S., 2005. Evidence for solar forcing of sea-surface temperature on the North Icelandic shelf during the late Holocene. *Geology* 33, 73–76.
- Jungclauss, J.H., Lorenz, S.J., Timmreck, C., Reick, C.H., Brovkin, V., Six, K., Segschneider, J., Giorgetta, M.A., Crowley, T.J., Pongratz, J., Krivova, N.A., Vieira, L.E., Solanki, S.K., Klocke, D., Botzet, M., Esch, M., Gayler, V., Haak, H., Raddatz, T.J., Roeckner, E., Schnur, R., Widmann, H., Claussen, M., Stevens, B., Marotzke, J., 2010. Climate and carbon-cycle variability over the last millennium. *Clim. Past* 6, 723–737.
- Kalnay, E., 2003. *Atmospheric Modeling, Data Assimilation and Predictability*. Cambridge University Press, Cambridge, United Kingdom. 339 pp.
- Kaplan, J.O., Krumhardt, K.M., Zimmermann, N., 2009. The prehistoric and preindustrial deforestation of Europe. *Quatern. Sci. Rev.* 28, 3016–3034.
- Klimenko, V.V., Klimanov, V.A., Sirin, A.A., Sleptsov, A.M., 2001. Climate changes in Western European Russia in the late Holocene. *Dokl. Earth Sci.* 377 (2), 190–194.
- Kremenetski, K.V., Boettger, T., MacDonald, G.M., Vaschalova, T., Sulerzhitsky, L., Hiller, A., 2004. Medieval climate warming and aridity as indicated by multiproxy evidence from the Kola Peninsula, Russia. *Palaeogeogr. Palaeoclimatol. Palaeoecol.* 209, 113–125.
- Lamb, H.H., 1965. The early Medieval warm epoch and its sequel. *Palaeogeogr. Palaeoclimatol. Palaeoecol.* 1, 13–37.
- Lean, J.L., Wang, Y.-M., Sheeley, N.R., 2002. The effect of increasing solar activity on the Sun's total and open magnetic flux during multiple cycles: implications for solar forcing of climate. *Geophys. Res. Lett.* 29 (24), 2224.
- Luterbacher, J., Dietrich, D., Xoplaki, E., Grosjean, M., Wanner, H., 2004. European seasonal and annual temperature variability, trends, and extremes since 1500. *Science* 303, 1499–1503.
- Mangini, A., Spötl, C., Verdes, P., 2005. Reconstruction of temperature in the Central Alps during the past 2000 yr from a $\delta^{18}\text{O}$ stalagmite record. *Earth Planet. Sci. Lett.* 235, 741–751.
- Mann, M.E., Rutherford, S., Wahl, E., Ammann, C., 2007. Robustness of proxy-based climate field reconstruction methods. *J. Geophys. Res.* 112, D12109. doi:10.1029/2006JD008272.
- Mann, M.E., Zhang, Z., Hughes, M.K., Bradley, R.S., Miller, S., Rutherford, S., Ni, F., 2008. Proxy-based reconstructions of hemispheric and global surface temperature variations over the past two millennia. *Proc. Natl. Acad. Sci. U. S. A.* 105, 13252–13257.
- Mann, M.E., Zhang, Z.H., Rutherford, S., Bradley, R.S., Hughes, M.K., Shindell, D., Ammann, C., Faluvegi, G., Ni, F.B., 2009. Global signatures and dynamical origins of the little ice age and medieval climate anomaly. *Science* 326, 1256–1260.
- Matthews, H.D., Weaver, A.J., Meissner, K.J., Gillet, N.P., Eby, M., 2004. Natural and anthropogenic climate change: incorporating historical land cover change, vegetation dynamics and the global carbon cycle. *Clim. Dyn.* 22, 461–479.
- Muscheler, R., Joos, F., Beer, J., Muller, S.A., Vonmoos, M., Snowball, I., 2007. Solar activity during the last 1000 yr inferred from radionuclide records. *Quatern. Sci. Rev.* 26, 82–97.
- Opsteegh, J.D., Haarsma, R.J., Seltén, F.M., Kattenberg, A., 1998. ECBilt: a dynamic alternative to mixed boundary conditions in ocean models. *Tellus* 50A, 348–367.

- Pfister, C., Luterbacher, J., Schwarz-Zanetti, G., Wegmann, M., 1998. Winter air temperature variations in Western Europe during the Early and high Middle Ages (AD 750–1300). *Holocene* 8, 535–552.
- Pitman, A.J., de Noblet-Ducoudré, N., Cruz, F.T., Davin, E.L., Bonan, G.B., Brovkin, V., Claussen, M., Delire, C., Ganzeveld, L., Gayler, V., van den Hurk, B.J.J.M., Lawrence, P.J., van der Molen, M.K., Müller, C., Reick, C.H., Seneviratne, S.I., Strengers, B.J., Voldoire, A., 2009. Uncertainties in climate responses to past land cover change: First results from the LUCID intercomparison study. *Geophys. Res. Lett.* 36, L14814. doi:10.1029/2009GL039076.
- Pohlmann, H., Sienz, F., Latif, M., 2006. Influence of the multidecadal Atlantic meridional overturning circulation variability on European climate. *J. Clim.* 19, 6062–6067.
- Pongratz, J., Reick, C., Raddatz, T., Claussen, M., 2008. A reconstruction of global agricultural areas and land cover for the last millennium. *Glob. Biogeochem. Cycles* 22, GB3018. doi:10.1029/2007GB003153.
- Pongratz, J., Raddatz, T., Reick, C.H., Esch, M., Claussen, M., 2009. Radiative forcing from anthropogenic land cover change since AD 800. *Geophys. Res. Lett.* 36, L02709. doi:10.1029/2008GL036394.
- Pongratz, J., Reick, C.H., Raddatz, T., Claussen, M., 2010. Biogeophysical versus biogeochemical climate response to historical anthropogenic land cover change. *Geophys. Res. Lett.* 37, L08702. doi:10.1029/2010GL043010, 2010.
- Ramankutty, N., Foley, J.A., 1999. Estimating historical changes in global land cover: croplands from 1700 to 1992. *Glob. Biogeochem. Cycles* 13 (4), 997–1027.
- Richter, T.O., Peeters, F.J.C., van Weering, T.C.E., 2009. Late Holocene (0–2.4 ka BP) surface water temperature and salinity variability, FENI Drift, NE Atlantic Ocean. *Quatern. Sci. Rev.* 28, 1941–1955.
- Robock, A., 2000. Volcanic eruptions and climate. *Rev. Geophys.* 38, 191–219.
- Sansó, B., Foresty, C.E., Zantedeschiz, D., 2008. Inferring climate system properties using a computer model. *Bayesian Anal.* 3 (1), 1–38.
- Schmidt, G.A., Jungclaus, J.H., Ammann, C.M., Bard, E., Braconnot, P., Crowley, T.J., Delaygue, G., Joos, F., Krivova, N.A., Muscheler, R., Otto-Bliesner, B.L., Pongratz, J., Shindell, D.T., Solanki, S.K., Steinhilber, F., Vieira, L.E.A., 2010. Climate forcing reconstructions for use in PMIP simulations of the last millennium (v1.0). *Geosci. Model Dev. Discuss.* 3, 1549–1586.
- Semenov, V.A., Latif, M., Dommenges, D., Keenlyside, N.S., Strehz, A., Martin, T., Park, W., 2010. The impact of north Atlantic–Arctic multidecadal variability on northern hemisphere surface air temperature. *J. Clim.* 23, 5668–5677.
- Seppä, H., Björne, A.E., Telford, R.J., Birks, H.J.B., Veski, S., 2009. Last nine-thousand years of temperature variability in Northern Europe. *Clim. Past* 5, 523–535.
- Servonnat, J., 2011. Variabilité climatique en Atlantique Nord au cours du dernier millénaire: évaluation de l'influence du forçage solaire avec le mode IPSLCM4. PhD thesis, Université de Versailles-St Quentin en Yvelines, 224 pp.
- Servonnat, J., Yiou, P., Khodri, M., Swingedouw, D., Denvil, S., 2010. Influence of solar variability CO2 and orbital forcing between 1000 and 1850 AD in the IPSLCM4 model. *Clim. Past* 6, 445–460.
- Shabalova, M.V., Van Engelen, F.V., 2003. Evaluation of a reconstruction of winter and summer temperatures in the low countries, AD 764–1998. *Clim. Change* 58, 219–242.
- Shapiro, A.I., Schmutz, W., Rozanov, E., Schoell, M., Haberleiter, M., Shapiro, A.V., Nyeki, S., 2011. A new approach to long-term reconstruction of the solar irradiance leads to large historical solar forcing. *Astron. Astrophys.* 529, A67. doi:10.1051/0004-6361/201016173.
- Shindell, D.T., Schmidt, G.A., Mann, M.E., Rind, D., Waple, A., 2001. Solar forcing of regional climate change during the Maunder Minimum. *Science* 294, 2149–2152.
- Shindell, D.T., Schmidt, G.A., Miller, R., Mann, M.E., 2003. Volcanic and solar forcing of climate change during the pre-industrial era. *J. Clim.* 16, 4094–4107.
- Sicre, M.A., Jacob, J., Ezat, U., Rousse, S., Kissel, C., Yiou, P., Eiriksson, J., Knudsen, K.L., Jansen, E., Turon, J.L., 2008. Decadal variability of sea surface temperatures off North Iceland over the last 2000 years. *Earth Planet. Sci. Lett.* 268, 137–142.
- Smerdon, J.E., Kaplan, A., Zorita, E., González-Rouco, J.F., Evans, M.N., 2011. Spatial performance of four climate field reconstruction methods. *Geophys. Res. Lett.* 38, L11705. doi:10.1029/2011GL047372.
- Snyder, C., Bengtsson, T., Bickel, P., Anderson, J., 2008. Obstacles to high-dimensional particle filtering. *Mon. Weather Rev.* 135, 4629–4640.
- Sutton, R., Hodson, D., 2005. Atlantic Ocean forcing of North American and European summer climate. *Science* 309, 115–118.
- Swingedouw, D., Terray, L., Cassou, C., Voldoire, A., Salas-Méla, D., Servonnat, J., 2010. Natural forcing of climate during the last millennium: fingerprint of solar variability. *Clim. Dyn.* doi:10.1007/s00382-010-0803-5
- Tiljander, M., Saarnisto, M., Ojala, A.K., Saarinen, T., 2003. A 3000-year paleoenvironmental record from annually laminated sediment of Lake Korttajärvi, central Finland. *Boreas* 32, 567–577.
- Timmreck, C., Lorenz, S.J., Crowley, T.J., Kinne, S., Raddatz, T.J., Thomas, M.A., Jungclaus, J.H., 2009. Limited temperature response to the very large AD 1258 volcanic eruption. *Geophys. Res. Lett.* 36, L21708. doi:10.1029/2009GL040083.
- Trouet, V., Esper, J., Graham, N., Baker, A., Scourse, J.D., Frank, D.C., 2009. Persistent positive North Atlantic Oscillation mode dominated the Medieval Climate anomaly. *Science* 324, 78–80.
- van der Schrier, G., Barkmeijer, J., 2005. Bjerknes' hypothesis on the coldness during AD 1790–1820 revisited. *Clim. Dyn.* 24, 335–371.
- van Engelen, A.F.V., Buisman, J., Ijnsen, F., 2001. A millennium of weather, winds and water in the low countries. In: Jones, P.D., et al. (Ed.), *History and Climate: Memories of the Future?* Kluwer Acad., Dordrecht, The Netherlands, pp. 101–124.
- van Leeuwen, P.J., 2009. Particle filtering in geophysical systems. *Mon. Weather Rev.* 137, 4089–4114.
- Wanner, H., Brönnimann, S., Casty, C., Gyalistras, D., Luterbacher, J., Schmutz, C., Stephenson, D.B., Xoplaki, E., 2001. North Atlantic oscillation – concepts and studies. *Surv. Geophys.* 22, 321–382.
- Widmann, M., Goosse, H., van der Schrier, G., Schnur, R., Barkmeijer, J., 2010. Using data assimilation to study extratropical Northern Hemisphere climate over the last millennium. *Clim. Past* 6, 627–644.